Am J Transl Res 2022;14(8):5896-5904
www.ajtr.org /ISSN:1943-8141/AJTR0144968

Original Article

Autophagy genes CCL2 and MYC are considered as potential biomarkers for pulmonary embolism

Xuehui Zhang[1*], Naibin Yang[2*], Lijiang Shao[3], Xuxia Chen[3], Xueqin Chen[4]

[1]Department of General Practice, Ningbo First Hospital, No. 59 Liuting Street, Haishu District, Ningbo, Zhejiang Province, P. R. China; [2]Department of Infectious Disease, Ningbo First Hospital, No. 59 Liuting Street, Haishu District, Ningbo, Zhejiang Province, P. R. China; [3]Department of Emergency, Ningbo First Hospital, No. 59 Liuting Street, Haishu District, Ningbo, Zhejiang Province, P. R. China; [4]Hospital Quality Management Office, Ningbo First Hospital, No. 59 Liuting Street, Haishu District, Ningbo, Zhejiang Province, P. R. China. [*]Equal contributors and co-first authors.

Received June 27, 2022; Accepted July 19, 2022; Epub August 15, 2022; Published August 30, 2022

Abstract: Objective: The pathogenesis of pulmonary embolism (PE) remains unclear. This study was designed to determine the differential genes associated with PE autophagy via the gene expression omnibus (GEO). Methods: Microarray data sets GSE11851 and GSE13535 were downloaded from the GEO to determine the differentially expressed genes (DEGs) of PE, and the protein-protein interaction (PPI) and hub gene networks were constructed by string and Cytoscape software. Additionally, the two data sets were screened to find the autophagy-related genes with common differential expression. Then, autophagy-related hub genes (ARHGs) overlapping with autophagy-related genes and hub genes were identified. Next, the mRNA-miRNA network was constructed, and finally the expressions of hub genes were determined with GSE11851 and GSE13535. Results: A total of 235 common DEGs were identified, and C-C motif chemokine ligand 2 (CCL2) and MYC proto-oncogene (MYC) were identified to be the ARHGs of PE. Additionally, a co-expression network of mRNAs and miRNAs, consisting of 94 nodes and 103 edges, was constructed by Cytoscape. PE samples showed significantly higher expressions of CCL2 and MYC than the control samples ($P < 0.05$). According to gene set enrichment analysis (GSEA), CCL2 was closely correlated with oxidative stress and inflammatory reaction, while MYC was closely correlated with inflammatory reaction. Conclusion: According to analysis, CCL2 and MYC, with high expression in PE samples, are promising potential markers of PE.

Keywords: Autophagy, CCL2, MYC, pulmonary embolism

Introduction

Pulmonary embolism (PE) refers to the clinical and pathophysiological syndrome in which the thrombus in the right heart or venous system blocks the main trunk of pulmonary artery or its branches and causes pulmonary circulation disorder [1, 2], with characteristics of high incidence, high missed diagnosis rate and high mortality [3]. PE has become a major health care problem that seriously endangers patients' quality of life. However, its pathogenesis is still yet to be determined. Therefore, clarifying its pathogenesis is of profound significance for the diagnosis and treatment of PE.

PE usually triggers severe hypoxia, lung ischemia and lung injury, but clinically, less than 10% of patients with PE suffer secondary lung infarction [4], which has aroused widespread concern of scholars [4]. Currently, the research on the mechanism of lung injury mostly focuses on injury and oxidative stress. It is considered that the central link of this kind of injury is the production of a large number of reactive oxygen species (ROS), which results in a series of chain reactions such as neutrophil activation, inflammatory mediator production and protease increase, and apoptosis and necrosis are considered as pathological outcomes of ischemic tissue cells [5, 6]. As research deepens, it has been found that ROS not only participates in the process of apoptosis, but also plays a crucial role in autophagy induction as a signal molecule [7]. Autophagy is a cellular process that

Table 1. Details of PE-associated data in GEO

Accession	Platform	Sample	Control	Pulmonary embolism
GSE13535	GPL1355	Rat	6	16
GSE11851	GPL1355	Rat	10	10

promotes the degradation of lysosomes of long-lived cytoplasmic proteins. It is initiated in the process of differentiation, nutritional deficiency or cell stress (including oxidative stress, endoplasmic reticulum stress and aggregation of protein aggregates) [8, 9]. Reportedly, both exposure to pharmacological autophagy inhibitors, 3-methyladenine (3-MA) and bafimycin A1 (Baf-A1) and gene deletions such as platelet-specific atg5 and atg7-or Becn+/- will damage platelet aggregation, hemostasis and thrombosis [10], and hypoxic preconditioning can induce platelet mitochondrial autophagy, reducing the heart injury due to ischemia/reperfusion [11]. These findings suggest that platelet mitochondrial autophagy can protect platelets from oxidative stress-induced damage, thus preventing platelet activation and thrombosis.

Over the past few years, amid a rise of autophagy and apoptosis research, some scholars have suggested that autophagy and apoptosis play a crucial role in the lung protective effect against PE [12]. However, there are few studies on the correlation and mechanism of PE with autophagy and apoptosis. Accordingly, this study conducted a series of analyses to determine the role of PE autophagy, which could play a possible role in the diagnosis and treatment of PE.

Methods and data

Data gathering

A total of 221 autophagy-related genes were acquired from the Autophagy Database (http://www.tanpaku.org/autophagy/). The mRNA expression profile data sets (GSE11851 and GSE13535) were downloaded from Gene Expression Omnibus (GEO) (https://www.ncbi.nlm.nih.gov/geo/). The two data sets were both located on GPL1355 platform. ID was converted into Symbol ID, and when multiple probes corresponded to one gene, the average expression value was taken as the gene expression value. Before analysis, log2 conversion and quantile normalization were conducted on the original data. Details of the two data sets are shown in **Table 1**.

Analysis of differential gene expression

The normalized expression matrix of microarray data was downloaded from the two datasets and represented by a box diagram. Then the annotation file in the datasets was adopted to annotate the probe. The reproducibility of data was verified by principal component analysis (PCA), and the PCA diagram was drawn by R package ggord. The matrix was analyzed by "limma" in the R software, and genes with adjusted *P* value less than 0.05 and absolute folding change (FC) greater than 1 were regarded as differentially expressed genes (DEGs). The "heat map" and "ggplot2" software packages (version 3.3.3) in the R software (version 3.6.3) were adopted to create heat map, volcano map and block diagram.

Protein-protein interaction (PPI) analysis and correlation analysis of DEGs

The string database was adopted to analyze PPI network (https://string-db.org/) of DEGs. The data for gene analysis were imported using Cytoscape software (version 3.8.1), and genes with the top 20 scores were marked as central genes by MCC algorithm of Cytoscape plug-in. The human autophagy database was used to match hub genes, and then the genes overlapping with autophagy-related genes and hub genes were identified.

Construction of mRNA-miRNA regulatory network

With the starBase database (https://starbase.sysu.edu.cn/), the interaction between differentially expressed miRNAs and differentially expressed mRNAs were predicted. Then, the mRNA-miRNA regulatory network was established to describe the interaction between mRNAs and miRNAs as a potential target of PE. The Cytoscape software was used to visually adjust the network.

Gene set enrichment analysis (GSEA)

In order to explore the biological signal pathway, GSEA was carried out. According to the net enrichment fraction (NES), gene ratio and

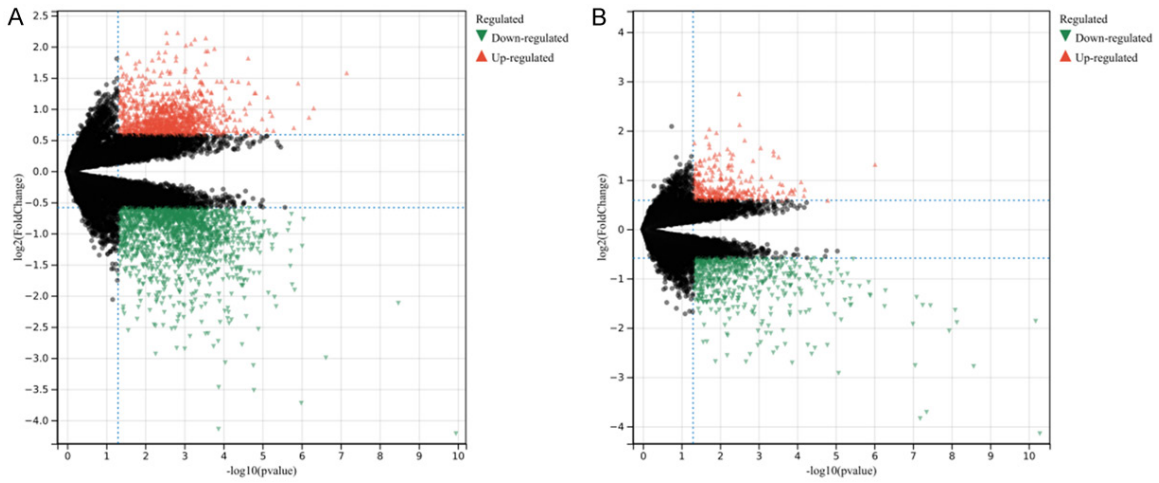

Figure 1. Volcano map of GSE11851 and GSE13535. A: Volcano map of differentially expressed genes in GSE11851 based on Limma analysis. B: Volcano map of differentially expressed genes in GSE13535 based on Limma analysis.

P value, Kyoto Encyclopedia of Genes and Genomes (KEGG) pathway was verified to have a significant enrichment effect, and |NES| > 0.5 and FDR q < 0.25 were considered as significant enrichment.

Statistical analysis

In the present study, GraphPad Prism 7 and R software (version 4.2.1) were adopted for statistical analysis. The data were expressed as the mean ± standard deviation, and compared between groups using the unpaired Student t test. P < 0.05 was considered statistically significant.

Results

Normalization analysis of data set

The expression matrices of the two datasets GSE11851 and GSE13535 were normalized, and the distribution trends in the block diagrams were basically a straight line (Figure S1A, S1B).

Screening of differential PE genes

According to the threshold of |log2(FC)| > 0.5 and *P* value < 0.05, 2662 differential genes were screened from the GSE11851 dataset (1605 genes downregulated and 1057 genes upregulated). A total of 855 DEGs were selected from the GSE13535 dataset (553 genes downregulated and 302 genes upregulated). The genes with top 10 highest and lowest differential expressions, respectively, in the two datasets were summarized in Tables S1, S2. In addition, corresponding volcano maps and heat maps were drawn (**Figures 1A**, **1B**, **2A**, **2B**).

Screening of autophagy-related hub genes (ARHGs)

Firstly, the common DEGs in the GSE11851 and GSE13535 datasets were analyzed. According to the Venn diagram, there were 235 common DEGs in the two datasets (**Figure 3A**). Then, the interaction between the above-mentioned DEGs was determined by PPI network. With Cytoscape software (version 3.8.1) for importing, the genes with the top 20 scores were marked as central genes. At last, IL1β, IL6, CCL2, TLR2, CXCL1, CD86, PTGS2, FN1, TP53, CCR1, TLR7, TIMP1, CD44, SERPINE1, MYD88, TYROBP, TLR1, CD14, MYC and FCGR2β were identified as the hub genes of PE (**Figure 3B**). Next, the expression of 221 autophagy-related genes in two datasets were analyzed, and the autophagy-related genes were determined by the adjusted criteria of |log2(FC)| > 0.5 and *P* value < 0.05. Venn diagram-based analysis of the two datasets identified the following DEGs (CCL2, MYC and SIRT1) in autophagy (**Figure 3C**). Interestingly, CCL2 was found by Venn map, and MYC was found in PE hub gene (**Figure 3D**). Finally, CCL2 and MYC were determined as ARHGs.

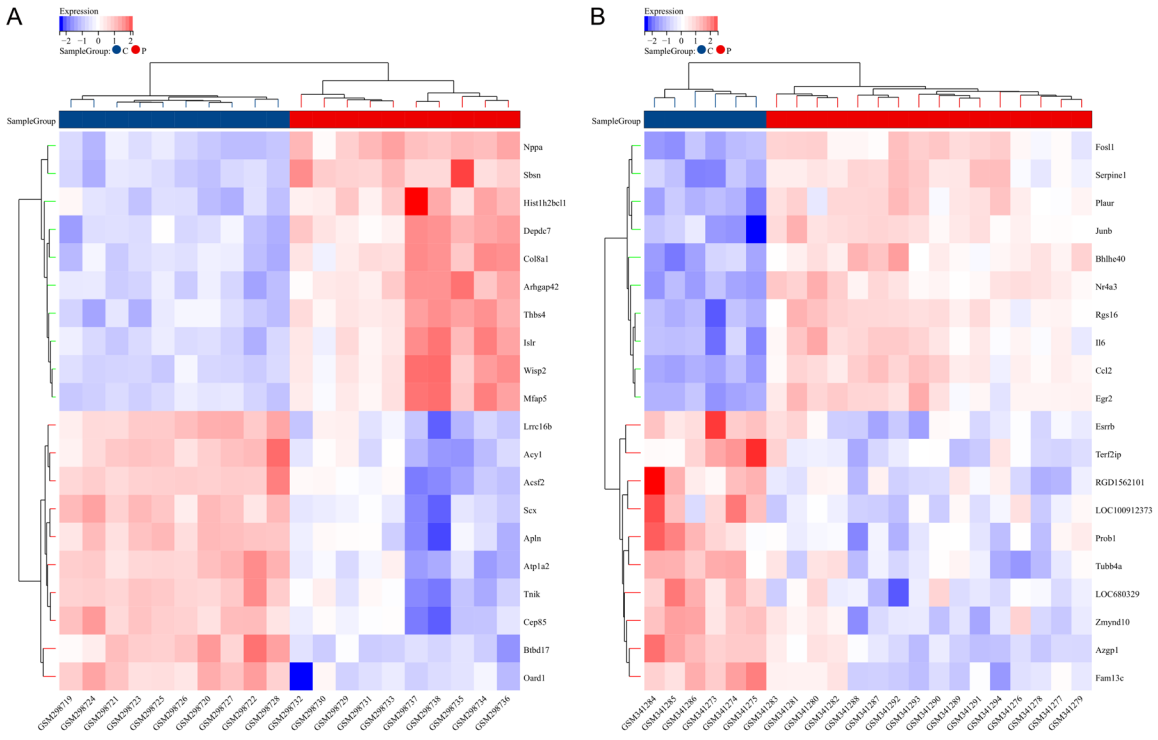

Figure 2. Heat map of GSE11851 and GSE13535. A. Heat map of differentially expressed genes in GSE11851 based on Limma analysis. B. Heat map of differentially expressed genes in GSE13535 based on Limma analysis. Note: C represents the control, and P represents the pulmonary embolism.

Construction of mRNA-miRNA network for ARHGs of APR

The starBase tool was adopted to predict the target miRNAs of hub genes. Finally, 94 targeted miRNAs were acquired, and 103 mRNA-miRNA pairs were determined, of which 9 shared target miRNA9. According to the prediction results, a mRNAs and miRNAs co-expression network (**Figure 4**) consisting of 94 nodes and 103 edges was constructed with Cytoscape (**Figure 4**).

Expressions of CCL2 and MYC in samples and GESA analysis

The expressions of CCL2 and MYC in the two datasets were further compared. According to the results, PE samples showed higher expressions of CCL2 and MYC than the control samples (**Figure 5A**, $P < 0.05$). In order to further determine the potential functions of CCL2 and MYC, GSEA analysis was conducted. Through Hallmark and KEGG functional analysis, CCL2 was found to be strongly related with oxidative stress and inflammatory reaction (**Figure 5B**, **5C**), and MYC was closely related with inflammatory reaction (**Figure 5D**, **5E**).

Discussion

PE is common, but its diagnosis is still elusive, so it is imperative to maintain a high degree of clinical suspicion when treating patients with cardiopulmonary symptoms [13]. In the past ten years, the diagnostic algorithms and techniques are relatively stagnating. The computed pathology pulmonary pathology is still the main diagnostic tool, but it is not applicable to all suspected PE cases [14]. In addition, most clinical manifestations of PE are nonspecific, which may result in frequent misdiagnosis [15]. Because of the high mortality associated with PE, it is necessary to understand the pathogenesis of PE in order to identify potential therapeutic targets.

In this study, two key autophagy-related genes (CCL2 and MYC) were identified using the expression array datasets GSE11851 and GSE13535. As far as we know, this is the first report that autophagy-related genes are

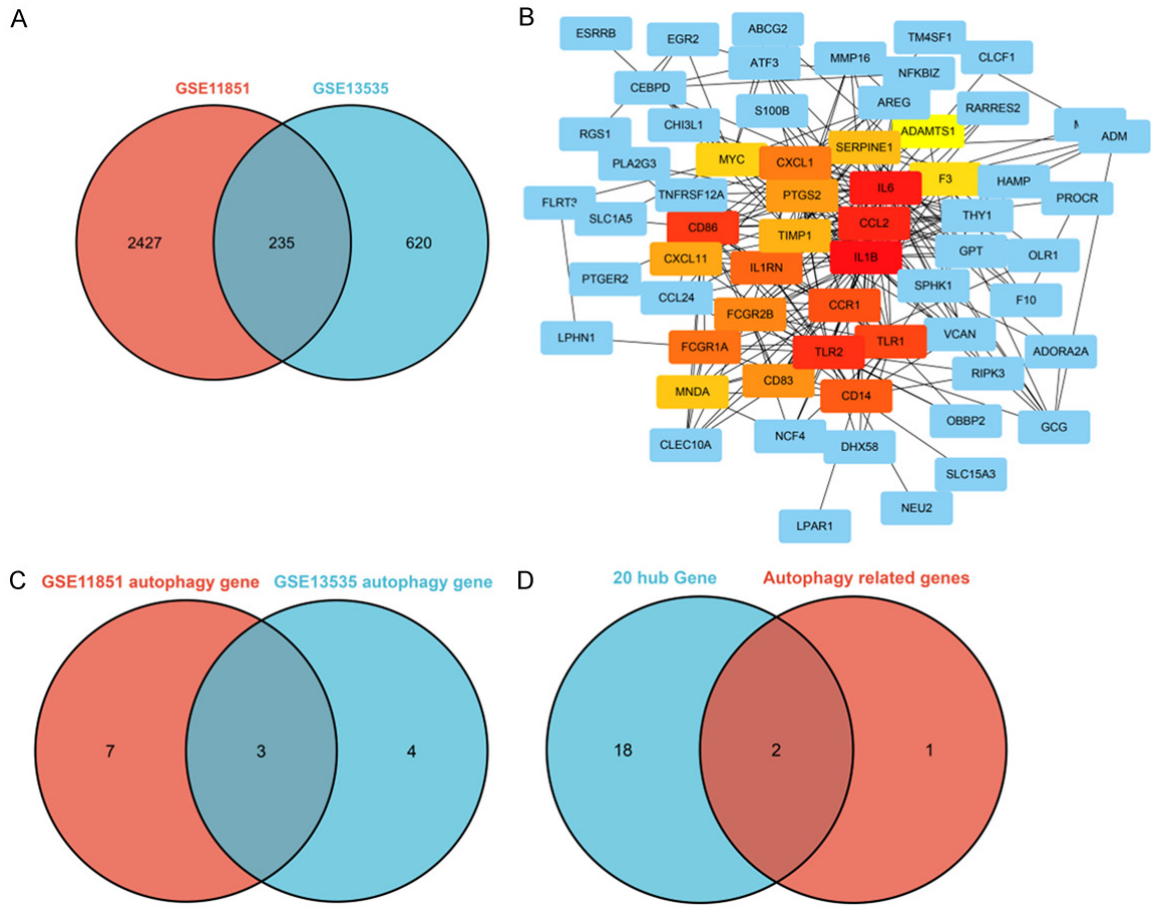

Figure 3. The DEGs in the GSE11851 and GSE13535 datasets and autophagy-related central genes. A: The common DEGs in the GSE11851 and GSE13535 datasets. B: The genes with the top 20 PPI scores were marked as central genes according to the Cytohubba plug-in. C: Venn diagram-based analysis of autophagy-related genes in two datasets. D: ARHGs. Note: differentially expressed genes (DEGs), Screening of autophagy-related hub genes (ARHGs), Protein-protein interaction (PPI).

involved in the occurrence and development of PE, and they are promising potential biomarkers in PE.

Autophagy is a kind of cell degradation and circulation process induced by various cell stress conditions, which is highly conservative in all eukaryotes and can protect cells [16]. Under normal physiological conditions, autophagy does not affect the survival and normal function of cells, but in the case of damage to the autophagy balance of cells *in vivo*, insufficient or excessive autophagy can cause abnormal cell function, leading to aggravation of pathological damage of related tissues and cells or even death [17-19]. Therefore, exploring the role of autophagy in the pathogenesis of PE may reveal a novel therapeutic method. For this reason, various array data in public databases, especially GEO, were adopted and subjected to bioinformatics analysis to explore and identify clinical biomarkers and potential therapeutic targets [20]. In the present study, the expression profiles and clinical information of patients with PE were downloaded from GEO, and two PE-related autophagy genes (CCL2 and MYC) were identified.

Chemokines belong to a superfamily of secreted proteins, which are involved in immune regulation and inflammatory processes [21]. CCL2 is a member of CC subfamily, with characteristics of two adjacent cysteine residues [22]. This cytokine has a chemotactic activity to monocytes and basophils, but no chemotactic activity to neutrophils and eosinophils [23]. Furthermore, CCL2 has been verified to promote inflammation, induce the release of other

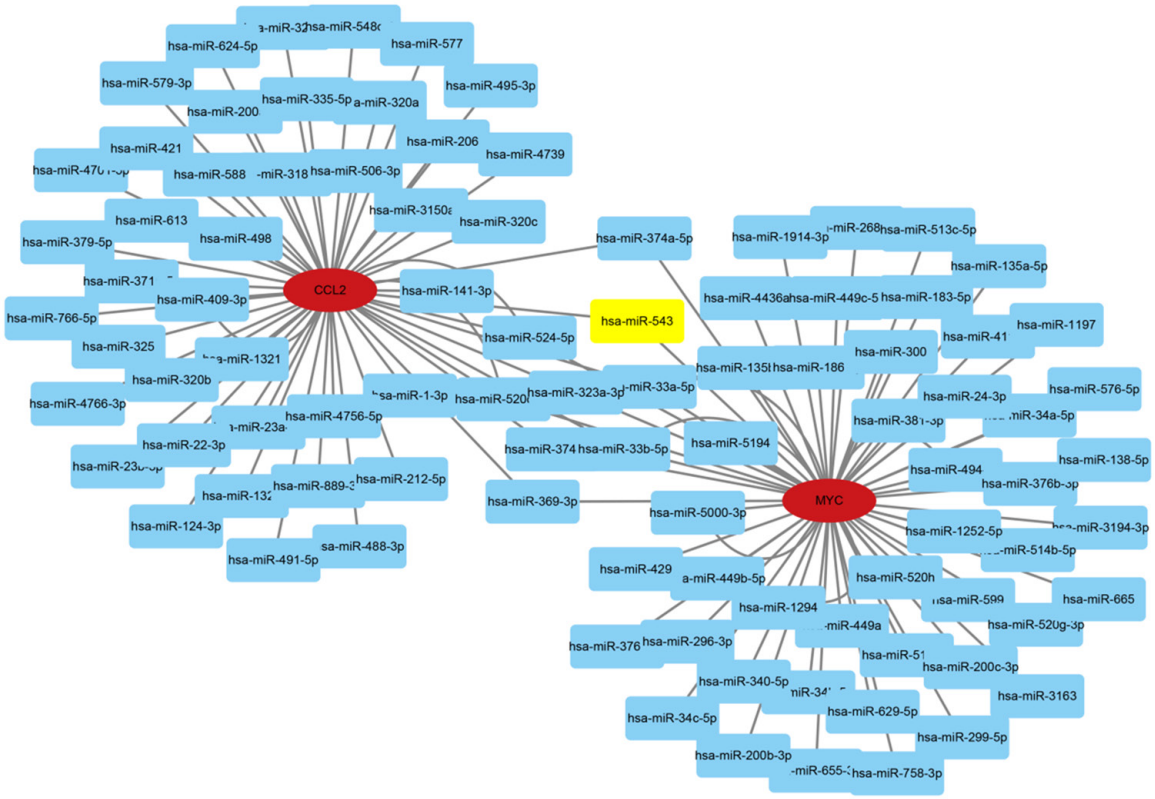

Figure 4. CCL2 and MYC gene can potentially bind microRNA. Note: C-C motif chemokine ligand 2 (CCL2) and MYC proto-oncogene (MYC).

inflammatory mediators to form positive feedback, and finally accelerate the progress of atherosclerosis [24]. CCL2 can also promote the directional migration of monocytes to atherosclerotic lesions by binding to its receptor CCR2. According to one study by Nieri et al. [25], with the increase of D-dimer level and the aggravation of gas exchange function, CCL2 level gradually increased, and the prognosis of patients with higher CCL2 level (> median) was significantly worse. In the present study, the expression of CCL2 in PE samples also increased, which suggested that CCL2 was strongly correlated with thrombosis.

MYC, also known as c-Myc, is a proto-oncogene that regulates cell cycle, apoptosis and cell transformation [26]. It is expressed in many human cancers such as breast cancer [27], lung cancer [28] and colorectal cancer [29]. Initial research showed that advanced c-Myc antisense (AVI-4126)-eluting phosphorylcholine-coated stent implantation was correlated with complete vascular healing and reduced neointimal formation in the porcine coronary restenosis model [30]. Studies by Tian et al. [31] found that c-Myc was positive in venular occlusion. Moreover, in the research by Li et al., carthamin yellow inhibited the expression of c-Myc in rats with PE, indicating the involvement of c-Myc in the occurrence and development of PE.

At the end of this study, the functions of CCL2 and MYC were analyzed according to GSEA. The results showed the involvement of abnormal expressions of CCL2 and MYC in peroxisome, inflammatory response, innate immune response and chemokine signaling pathway. We speculate that abnormal expressions of CCL2 and MYC are important genetic predictors of PE.

This study has confirmed that CCL2 and MYC are potential markers in PE through analysis, but it still has some limitations. First of all, we have not collected any clinical samples for verification as the analysis of health information. Secondly, we have not conducted basic research on its specific mechanism. Finally, more samples are required to verify whether CCL2 and MYC can be adopted as diagnostic indica-

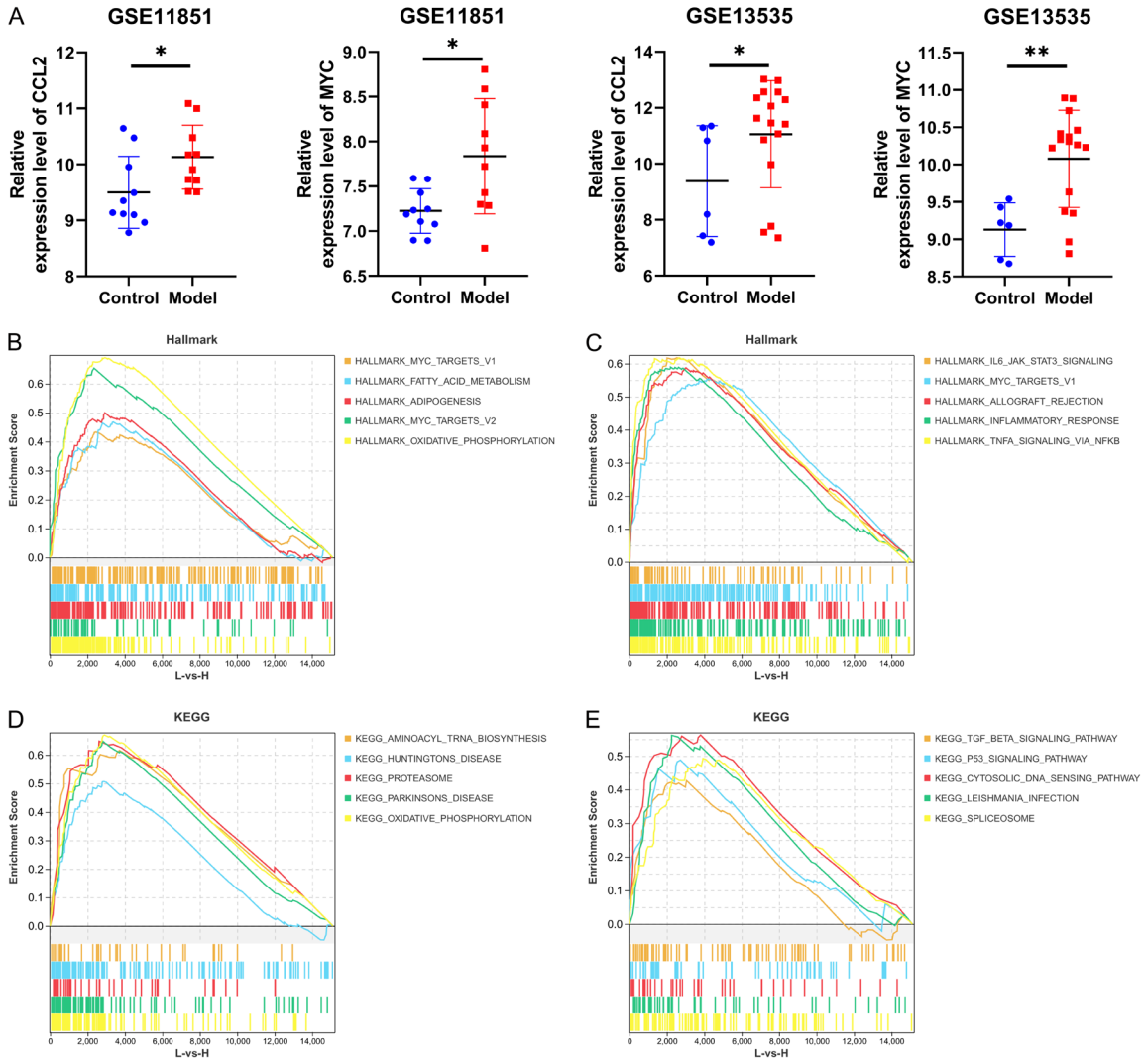

Figure 5. The expression and functional analysis of CCL2 and MYC in pulmonary embolism samples. A: The expression of CCL2 and MYC in GSE11851 and GSE13535 datasets. B: The Hallmark functional analysis of CCL2 single gene. C: The KEGG functional analysis of CCL2 single gene. D: The Hallmark functional analysis of MYC single gene. E: The KEGG functional analysis of MYC single gene. Note: C-C motif chemokine ligand 2 (CCL2) and MYC proto-oncogene (MYC), Kyoto Encyclopedia of Genes and Genomes (KEGG).

tors of PE. We hope to carry out prospective research in the future with a larger sample size to verify the research conclusions.

To sum up, according to analysis, CCL2 and MYC, with high expression in PE, are promising potential markers of PE.

Acknowledgements

This work was supported by Zhejiang Provincial Basic Public Welfare Research Project (No. Y19H010009) and Ningbo key technology research and development projects (No. 2021-Z018).

Disclosure of conflict of interest

None.

Address correspondence to: Xueqin Chen, Hospital Quality Management Office, Ningbo First Hospital, No. 59 Liuting Street, Haishu District, Ningbo, Zhejiang Province, P. R. China. Tel: +86-0574-87085020; E-mail: Cxq2316@163.com

References

[1] Doherty S. Pulmonary embolism an update. Aust Fam Physician 2017; 46: 816-820.
[2] Howard L. Acute pulmonary embolism. Clin Med (Lond) 2019; 19: 243-247.

[3] Giordano NJ, Jansson PS, Young MN, Hagan KA and Kabrhel C. Epidemiology, pathophysiology, stratification, and natural history of pulmonary embolism. Tech Vasc Interv Radiol 2017; 20: 135-140.
[4] Rivera-Lebron BN, Rali PM and Tapson VF. The PERT concept: a step-by-step approach to managing pulmonary embolism. Chest 2021; 159: 347-355.
[5] Cau SB, Barato RC, Celes MR, Muniz JJ, Rossi MA and Tanus-Santos JE. Doxycycline prevents acute pulmonary embolism-induced mortality and right ventricular deformation in rats. Cardiovasc Drugs Ther 2013; 27: 259-267.
[6] Mizera R. [Pathophysiology of development of pulmonary hypertension after acute pulmonary embolism]. Cesk Fysiol 2012; 61: 4-8.
[7] Luo Z, Xu X, Sho T, Zhang J, Xu W, Yao J and Xu J. ROS-induced autophagy regulates porcine trophectoderm cell apoptosis, proliferation, and differentiation. Am J Physiol Cell Physiol 2019; 316: C198-C209.
[8] Gao L, Loveless J, Shay C and Teng Y. Targeting ROS-mediated crosstalk between autophagy and apoptosis in cancer. Adv Exp Med Biol 2020; 1260: 1-12.
[9] Wang K. Autophagy and apoptosis in liver injury. Cell Cycle 2015; 14: 1631-1642.
[10] Lee TY, Lu WJ, Changou CA, Hsiung YC, Trang NTT, Lee CY, Chang TH, Jayakumar T, Hsieh CY, Yang CH, Chang CC, Chen RJ, Sheu JR and Lin KH. Platelet autophagic machinery involved in thrombosis through a novel linkage of AMPK-MTOR to sphingolipid metabolism. Autophagy 2021; 17: 4141-4158.
[11] Zhu H, Tan Y, Du W, Li Y, Toan S, Mui D, Tian F and Zhou H. Phosphoglycerate mutase 5 exacerbates cardiac ischemia-reperfusion injury through disrupting mitochondrial quality control. Redox Biol 2021; 38: 101777.
[12] Boulate D, Arthur Ataam J, Connolly AJ, Giraldeau G, Amsallem M, Decante B, Lamrani L, Fadel E, Dorfmuller P, Perros F, Haddad F and Mercier O. Early development of right ventricular ischemic lesions in a novel large animal model of acute right heart failure in chronic thromboembolic pulmonary hypertension. J Card Fail 2017; 23: 876-886.
[13] Konstantinides SV, Meyer G, Becattini C, Bueno H, Geersing GJ, Harjola VP, Huisman MV, Humbert M, Jennings CS, Jimenez D, Kucher N, Lang IM, Lankeit M, Lorusso R, Mazzolai L, Meneveau N, Ainle FN, Prandoni P, Pruszczyk P, Righini M, Torbicki A, Van Belle E and Zamorano JL; The Task Force for the diagnosis and management of acute pulmonary embolism of the European Society of Cardiology (ESC). 2019 ESC Guidelines for the diagnosis and management of acute pulmonary embolism developed in collaboration with the European Respiratory Society (ERS): The Task Force for the diagnosis and management of acute pulmonary embolism of the European Society of Cardiology (ESC). Eur Respir J 2019; 54: 1901647.
[14] Moore AJE, Wachsmann J, Chamarthy MR, Panjikaran L, Tanabe Y and Rajiah P. Imaging of acute pulmonary embolism: an update. Cardiovasc Diagn Ther 2018; 8: 225-243.
[15] Wang Y, Tan X, Gao H, Yuan H, Hu R, Jia L, Zhu J, Sun L, Zhang H, Huang L, Zhao D, Gao P and Du J. Magnitude of soluble ST2 as a novel biomarker for acute aortic dissection. Circulation 2018; 137: 259-269.
[16] Kocaturk NM, Akkoc Y, Kig C, Bayraktar O, Gozuacik D and Kutlu O. Autophagy as a molecular target for cancer treatment. Eur J Pharm Sci 2019; 134: 116-137.
[17] Li W, He P, Huang Y, Li YF, Lu J, Li M, Kurihara H, Luo Z, Meng T, Onishi M, Ma C, Jiang L, Hu Y, Gong Q, Zhu D, Xu Y, Liu R, Liu L, Yi C, Zhu Y, Ma N, Okamoto K, Xie Z, Liu J, He RR and Feng D. Selective autophagy of intracellular organelles: recent research advances. Theranostics 2021; 11: 222-256.
[18] Mizushima N and Levine B. Autophagy in human diseases. N Engl J Med 2020; 383: 1564-1576.
[19] Antunes F, Erustes AG, Costa AJ, Nascimento AC, Bincoletto C, Ureshino RP, Pereira GJS and Smaili SS. Autophagy and intermittent fasting: the connection for cancer therapy? Clinics (Sao Paulo) 2018; 73: e814s.
[20] Toro-Dominguez D, Martorell-Marugan J, Lopez-Dominguez R, Garcia-Moreno A, Gonzalez-Rumayor V, Alarcon-Riquelme ME and Carmona-Saez P. ImaGEO: integrative gene expression meta-analysis from GEO database. Bioinformatics 2019; 35: 880-882.
[21] Lim SY, Yuzhalin AE, Gordon-Weeks AN and Muschel RJ. Targeting the CCL2-CCR2 signaling axis in cancer metastasis. Oncotarget 2016; 7: 28697-28710.
[22] Xu M, Wang Y, Xia R, Wei Y and Wei X. Role of the CCL2-CCR2 signalling axis in cancer: Mechanisms and therapeutic targeting. Cell Prolif 2021; 54: e13115.
[23] Yang L, Li N, Yang D, Chen A, Tang J, Jing Y, Kang D, Jiang P, Dai X, Luo L, Chen Q, Chang J, Liu J, Gu H, Huang Y, Chen Q, Li Z, Zhu Y, Miller H, Chen Y, Qiu L, Mei H, Hu Y, Gong Q and Liu C. CCL2 regulation of MST1-mTOR-STAT1 signaling axis controls BCR signaling and B-cell differentiation. Cell Death Differ 2021; 28: 2616-2633.
[24] Gleissner CA, von Hundelshausen P and Ley K. Platelet chemokines in vascular disease. Arterioscler Thromb Vasc Biol 2008; 28: 1920-1927.

[25] Nieri D, Neri T, Barbieri G, Moneta S, Morelli G, Mingardi D, Spinelli S, Ghiadoni L, Falcone M, Tiseo G, Menichetti F, Franzini M, Caponi L, Paolicchi A, Pancani R, Pistelli F, Carrozzi L and Celi A; Pisa COVID group. C-C motive chemokine ligand 2 and thromboinflammation in COVID-19-associated pneumonia: a retrospective study. Thromb Res 2021; 204: 88-94.

[26] Farrell AS and Sears RC. MYC degradation. Cold Spring Harb Perspect Med 2014; 4: a014365.

[27] Fallah Y, Brundage J, Allegakoen P and Shajahan-Haq AN. MYC-Driven pathways in breast cancer subtypes. Biomolecules 2017; 7: 53.

[28] Park JE, Jung JH, Lee HJ, Sim DY, Im E, Park WY, Shim BS, Ko SG and Kim SH. Ribosomal protein L5 mediated inhibition of c-Myc is critically involved in sanggenon G induced apoptosis in non-small lung cancer cells. Phytother Res 2021; 35: 1080-1088.

[29] Butler DSC, Cafaro C, Putze J, Wan MLY, Tran TH, Ambite I, Ahmadi S, Kjellstrom S, Welinder C, Chao SM, Dobrindt U and Svanborg C. A bacterial protease depletes c-MYC and increases survival in mouse models of bladder and colon cancer. Nat Biotechnol 2021; 39: 754-764.

[30] Kipshidze NN, Iversen P, Kim HS, Yiazdi H, Dangas G, Seaborn R, New G, Tio F, Waksman R, Mehran R, Tsapenko M, Stone GW, Roubin GS, Iyer S, Leon MB and Moses JW. Advanced c-myc antisense (AVI-4126)-eluting phosphorylcholine-coated stent implantation is associated with complete vascular healing and reduced neointimal formation in the porcine coronary restenosis model. Catheter Cardiovasc Interv 2004; 61: 518-527.

[31] Tian ZL, Jia GL, Xi HL, Feng S, Wang XK and Li R. Investigation on etiology of hepatic venous obstruction Budd-Chiari syndrome. Cell Biochem Biophys 2014; 70: 1803-1806.

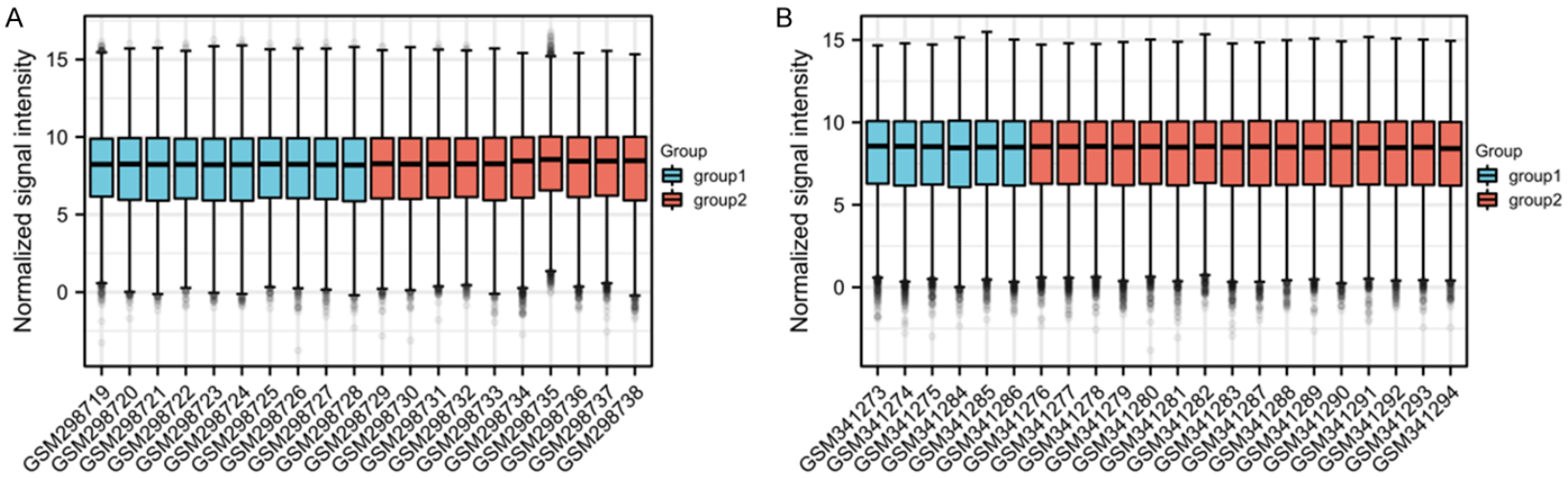

Figure S1. Processing of GEO data sets. A, B: Normalized expression matrix of datasets GSE11851 and GSE13535. A-Note: Gene Expression Omnibus (GEO).

Table S1. Top 10 DEGs in the GSE11851 dataset

Tag	logFC	AveExpr	t	*P*.Value	adj.*P*.Val	β
Down						
NPPA	-4.215	11.562	-12.223	1.117E-10	1.687E-06	13.643
RBP4	-4.144	5.807	-4.722	1.338E-04	5.774E-03	1.170
WISP2	-3.726	9.225	-6.946	1.016E-06	1.706E-03	5.724
LTBP2	-3.521	8.355	-5.642	1.660E-05	3.491E-03	3.129
CAR3	-3.471	7.475	-4.728	1.321E-04	5.748E-03	1.181
GLI1	-3.122	4.871	-5.628	1.715E-05	3.491E-03	3.099
SFRP2	-3.076	9.045	-4.895	8.988E-05	5.077E-03	1.544
THBS4	-2.998	7.734	-7.667	2.385E-07	9.009E-04	7.048
CIDEC	-2.935	4.320	-3.119	5.451E-03	2.730E-02	-2.300
C1QTNF3	-2.853	4.923	-3.865	9.797E-04	1.127E-02	-0.702
Up						
S100VP	2.413	1.882	4.731	1.311E-04	5.748E-03	1.188
CRYBB1	2.225	7.590	3.397	2.892E-03	1.873E-02	-1.713
MTTP	2.224	4.646	3.688	1.476E-03	1.359E-02	-1.085
LOC690326	2.140	5.398	4.399	2.830E-04	7.491E-03	0.465
SALL4	2.120	5.272	4.121	5.391E-04	9.256E-03	-0.141
TSGA13	2.062	2.828	3.419	2.750E-03	1.825E-02	-1.666
MAGIX	2.048	7.363	4.026	6.726E-04	9.849E-03	-0.349
FREM2	2.023	4.940	3.894	9.153E-04	1.097E-02	-0.638
ADRA1D	1.970	7.191	4.618	1.701E-04	6.217E-03	0.944
LOC102551306	1.932	2.529	4.452	2.499E-04	7.234E-03	0.581

Note: differentially expressed genes (DEGs).

Table S2. Top 10 DEGs in the GSE13535 dataset

Tag	logFC	AveExpr	t	*P*.Value	adj.*P*.Val	β
Down						
LTBP2	-4.149	10.601	-11.800	5.152E-11	4.991E-07	14.143
IL6	-3.843	6.605	-7.938	6.489E-08	9.804E-05	8.116
SERPINE1	-3.715	6.534	-8.122	4.429E-08	8.365E-05	8.454
TFPI2	-2.923	8.131	-5.756	8.479E-06	4.133E-03	3.701
RGS16	-2.786	8.651	-9.544	2.674E-09	1.347E-05	10.889
CXCL2	-2.767	8.461	-7.795	8.766E-08	1.104E-04	7.849
CCL7	-2.713	7.751	-4.608	1.351E-04	2.148E-02	1.139
SELE	-2.692	6.391	-3.478	2.124E-03	8.220E-02	-1.410
IL10	-2.686	3.838	-2.696	1.315E-02	1.715E-01	-3.067
ALDH1L2	-2.563	5.762	-3.003	6.525E-03	1.314E-01	-2.435
Up						
CYP1A1	4.225	6.818	3.710	1.212E-03	6.528E-02	-0.894
CPNE4	2.745	2.742	3.309	3.175E-03	9.973E-02	-1.779
BAAT	2.122	5.214	3.318	3.115E-03	9.928E-02	-1.761
BAI3	2.033	-0.012	2.532	1.895E-02	1.961E-01	-3.392
LOC100910231	1.959	5.211	2.724	1.236E-02	1.680E-01	-3.011
AQP11	1.880	3.170	2.447	2.283E-02	2.108E-01	-3.556
LONP1	1.806	1.338	3.445	2.298E-03	8.575E-02	-1.482
CWC25	1.752	7.109	2.113	4.612E-02	2.761E-01	-4.167
KCNJ1	1.733	1.910	2.526	1.919E-02	1.966E-01	-3.403
MCPT2	1.659	6.716	2.539	1.868E-02	1.945E-01	-3.379

Note: differentially expressed genes (DEGs).